The static water-contact angles of CLPE-*g*-MPC polymerized with various MPC concentrations were measured by a sessile drop method using an optical bench-type contact angle goniometer (Model DM300; Kyowa Interface Science Co., Ltd., Saitama, Japan). Drops of purified water (1 μL) were deposited onto the surface of CLPE-*g*-MPC, and the contact angles were directly measured by using a microscope after 60 s according to the ISO 15989 standard.[29] Fifteen replicate measurements were performed on each sample, and the average values were taken as contact angles.

The functional group vibrations of the CLPE-*g*-MPC surface polymerized with various MPC concentrations were examined by Fourier-transform infrared (FT-IR) spectroscopy using attenuated total reflection (ATR) equipment. FT-IR/ATR spectra were obtained in 32 scans over a range of 800 to 2000 cm^{-1} using an FT-IR analyzer (FT/IR615, JASCO International Co., Ltd., Tokyo, Japan) at a resolution of 4.0 cm^{-1}.

Cross-section of CLPE-*g*-MPC observed with a transmission electron microscope

A cross-section of the MPC polymer layer on the CLPE-*g*-MPC surface produced by various MPC concentrations was observed with a transmission electron microscope (TEM). The specimens were first embedded in epoxy resin, stained with ruthenium oxide vapor at room temperature, and then sliced into ultra-thin films (approximately 100-nm thick) by using a Leica Ultra Cut UC microtome (Leica Microsystems, Ltd., Wetzlar, Germany). A JEM-1010 electron microscope (JEOL, Ltd., Tokyo, Japan) was used for the TEM observation at an acceleration voltage of 100 kV.

Surface coated-area observations by fluorescence microscopy

We used rhodamine 6G (Wako Pure Chemical Industries, Ltd., Osaka, Japan) that can be applied simply and rapidly to a polymer coating and imaged using fluorescence microscopy. Wang et al. found that rhodamine 6G effectively stains poly(MPC) that possesses great structural similarity to lipids.[30]

An aqueous solution of 200 mass ppm rhodamine 6G was used for all the staining experiments. All the samples were stained by following a two-step procedure: (1) The samples were immersed in the rhodamine 6G solution for 30 s and then removed. (2) Next, they were washed two times consecutively in distilled water for 30 s and then dried.

A fluorescence microscope (Axioskop 2 Plus, Carl Zeiss AG, Oberkochen, Germany) was used for fluorescence microscopy imaging and examination of all samples. Pseudo-color images were obtained using a CCD camera (VB-7010, Keyence Co., Osaka, Japan) and imaging software (VH analyzer 2.51, Keyence Co.). Lenses with ×10 magnification and appropriate exposure time (approximately 1/10 s) were employed to obtain best image quality of the samples.

Friction test

The friction test was performed using a ball-on-plate machine (Tribostation 32; Shinto Scientific Co., Ltd., Tokyo, Japan). Six sample pieces were prepared using each CLPE-*g*-MPC with various MPC concentration. The Co-Cr-Mo alloy ball was 9 mm in diameter and its surface roughness was $Ra \geq 0.01$—as smooth as a femoral ball. The friction tests were carried out with a load of 0.98 N and a sliding distance of 25 mm with a frequency of 1 Hz at room temperature.[31] The measurements were performed using pure water as lubricant. The friction tests were performed up to a maximum of 100 cycles. The mean static (μ_s) and dynamic (μ_d) coefficients of friction were determined by averaging five data points in 100 (96–100) cycle measurements.

Hip simulation wear test

The CLPE and CLPE-*g*-MPC cups were 26 mm inner and 52 mm outer diameter for use in the hip joint simulator. For each MPC concentrations (0 (untreated), 0.25 and 0.50 mol/L), 2 pieces were prepared. The wear test was performed using a 12-station hip joint simulator (MTS Systems Corp., MN, USA). A Co-Cr-Mo alloy femoral ball component with a size of 26 mm (Japan Medical Materials Corp., Osaka, Japan) was used as an acetabular component. A mixture of 25vol% bovine serum, 20 mM/L of ethylene diamine tetraacetic acid (EDTA), and 0.1mass% sodium azide was used as lubricant, according to the ISO 14242-1 standard.[32] The lubricant was replaced every 0.5×10^6 cycles. Walks, simulating a physiologic loading curve (Paul-type) with double peaks of 1793 and 2744 N loads, were applied with multidirectional (biaxial and orbital) motion of 1 Hz frequency. The wear was determined by weighing the polyethylene cups. Load-soak controls (n = 2) were used to compensate the fluid absorption of specimens.[33] The weights of the cups were measured every 0.5×10^6 cycles. Then, the testing was continued until a total of 5.0×10^6 cycles were completed.

RESULTS

Fig. 1 shows the phosphorous concentration in the CLPE-*g*-MPC surface with various ultraviolet-ray irradiation times during polymerization. The phosphorous concentration increased as the irradiation time was increased. When the irradiation time was greater than 45 min, the phosphorous concentrations of the CLPE-*g*-MPC with 0.17, 0.25 and 0.50 mol/L MPC concentration became constant at the high values of 2.9, 3.8 and 4.6atom%, respectively.

Fig. 2 shows the content of nitrogen (N) and phosphorous (P) in the CLPE-*g*-MPC surface polymerized with various MPC concentrations and irradiation time (polymerization time) of 90 min. The content of nitrogen and phosphorous in the CLPE-*g*-MPC surface increased to 5.2 and 5.2, respectively, with up to 0.50 mol/L MPC concentrations, and then that gradually decreased with over the 0.67 mol/L MPC concentrations. The elemental composition of the CLPE-*g*-MPC surface with 0.50 mol/L MPC concentration was almost equivalent to the theoretical elemental composition (N = 5.3, P = 5.3) of MPC polymer.

Fig. 3 shows the static water-contact angle of CLPE-*g*-MPC as a function of the MPC concentration for polymerization (90 min irradiation). The static water-contact angle on the untreated CLPE was 90° and decreased markedly with an increase in the MPC concentration for polymerization. When the MPC concentration was between 0.25 and 0.50 mol/L, the static water-contact angle became constant at the low value of 15°.

Fig. 4 shows the FT-IR/ATR spectra of untreated CLPE and CLPE-*g*-MPC with various MPC concentrations during polymerization of 90 min. An absorption peak was observed at 1460 cm^{-1} for both CLPE and CLPE-*g*-MPC. This peak is attributed mainly to the methylene (CH_2) chain in the CLPE substrate and MPC graft polymer. However, transmission absorptions at 1240, 1080 and 970 cm^{-1} were observed only for the CLPE-*g*-MPC. These peaks are due to the phosphate group in the MPC unit. Similarly, an absorption peak at 1720 cm^{-1} observed for CLPE-*g*-MPC can only correspond to the carbonyl in the MPC unit. The absorption peak intensity attributed to the phosphate group increased with the MPC concentrations during polymerization to reach a maximum at 0.5 mol/L MPC concentrations.

Fig. 5 shows cross-sectional TEM images of CLPE-*g*-MPC produced with various MPC concentrations during polymerization of 90 min. With MPC concentrations higher than 0.25 mol/L, a grafted poly(MPC) layer 10 to 250-nm thick was clearly observed on the surface of the CLPE substrate. The MPC-covered region was coexistent with uncovered regions with MPC concentration of 1.0 mol/L, although the thickness on the poly(MPC) layer of the covered region showed the thickest of 200 to 250 nm. With MPC concentration of <0.06 mol/L, no poly(MPC) layer was observed on the surface of the CLPE (data not shown). These results indicate that the length of the grafted poly(MPC) chain (thickness of poly(MPC) layer) can be controlled by the MPC concentration during polymerization. This is attributable to the fact that the length of polymer chains produced in a radical polymerization reaction is generally correlated with the MPC concentration.

Fig. 6 shows the FM images of the CLPE-*g*-MPC surface with 0.50 and 1.00 mol/L MPC concentrations for polymerization of 90 min. On the CLPE-*g*-MPC surface with 0.50 mol/L MPC concentrations, the poly(MPC) layer stained with rhodamine 6G was more clearly visible, the staining was uniform. On the CLPE-*g*-MPC surface with 1.00 mol/L MPC concentrations, the untreated CLPE (unstained) surface was observed. It therefore indicates that the grafting of the poly(MPC) layer on the CLPE surface is not uniform. The several lines are machining marks in the FM images.

The static and dynamic coefficients of friction of CLPE-*g*-MPC produced with various MPC concentrations during polymerization of 90 min are shown in Fig. 7. Both the static and dynamic coefficients of friction of CLPE-*g*-MPC decreased markedly with an increase to 0.50 mol/L of the MPC concentration for polymerization, but those finally increased with over the 0.67 mol/L. When the MPC concentration was between 0.25 and 0.50 mol/L, the dynamic coefficients of friction became constant at the low values of 0.15 to 0.18. Considering the CLPE-*g*-MPC as regarding the MPC

concentration of 0.25 and 0.50 mol/L, approximately 80% reduction (i.e., 75 to 80%) was observed in the dynamic coefficients of friction when compared with those of untreated CLPE. Fig. 8 shows a relationship between the dynamic coefficient of friction and contact angle. The dynamic coefficient of friction depended on the contact angle. The line was straight to a degree of accuracy, their correlation coefficients being 0.920.

Fig. 9 shows the gravimetric wear of the untreated CLPE and CLPE-*g*-MPC cups with 0.50 and 1.00 mol/L MPC concentrations for polymerization of 90 min during the hip joint simulation test. The CLPE-*g*-MPC cups were found to wear significantly less than the untreated CLPE cups. There was not significantly different between wear of CLPE-*g*-MPC cup with 0.50 mol/L MPC concentration and that with 1.00 mol/L MPC concentration. The CLPE-*g*-MPC cups exhibited a slight increase in weight; this was attributable to slightly enhanced fluid absorption over and above the fluid absorption by the load-soak controls. When using the gravimetric method, we corrected the weight loss for the fluid absorption by subtracting the weight gain that occurred in the load-soak controls. Since the wear cups are subjected to motion and load, there are limitations to this correction; therefore, they are observed to absorb slightly more fluid than their load-soak controls. However, as a result, the correction for fluid absorption by using the load-soak controls data as the correction factor leads to a slight underestimation of the actual weight loss.[12, 33] We defined the steady wear rate as that from 4.0×10^6 to 5.0×10^6 cycles. The steady wear rate of the untreated CLPE cups was 5.11 mg/10^6 cycles. In contrast, the wear rates of the CLPE-*g*-MPC cups with 0.25 and 0.50 mol/L MPC concentrations were markedly lower at 0.12 and 0.32 mg/10^6 cycles, respectively.

DISCUSSION

We investigated the properties of the poly(MPC) layer formed on the CLPE surface with various MPC concentrations by photo-induced radical graft polymerization; this report discusses the wear resistant properties of CLPE-*g*-MPC in terms of the characteristics of the poly(MPC) nano-scale layer.

In Fig. 2, the content of nitrogen and phosphorous in the CLPE-*g*-MPC surface attributed to poly(MPC) increased to 5.2 and 5.2, respectively, with an increase of MPC concentration for polymerization. And in the TEM images as shown in Fig. 5, the thickness of poly(MPC) layer increased with an increase of MPC concentration. When the poly(MPC) layer has a brush like structure, the layer thickness might depend on the molecular weight of grafted poly(MPC). In the CLPE-*g*-MPC cups with a high-density poly(MPC) graft chains, the poly(MPC) graft chains are assumed to stand up to exhibit a brush like structure.[34, 35] And, it is generally well-known that the reaction rate of radical polymerization is extremely high.[36] It was considered that the length (molecular weight) of the poly(MPC) graft chain can be controlled by the MPC concentration during polymerization, and those results indicate that poly(MPC) chain grafted on the CLPE surface became

longer with an increase in MPC concentration for polymerization.[37] This is attributable to the fact that the length of polymer chains produced in a radical polymerization reaction is generally correlated with the MPC concentration. For the CLPE-*g*-MPC, the molecular weight of the grafted poly(MPC) is not available due to the difficulty in separating the grafted poly(MPC) from the CLPE substrate. Further efforts are needed in this aspect.

In the TEM observation, the thickest poly(MPC) layer (200 to 250 nm) was observed on the surface of CLPE-*g*-MPC surface with 1.00 mol/L MPC concentrations (Fig. 5(d)). However, the content of nitrogen and phosphorous in the CLPE-*g*-MPC surface determined by XPS analysis, decreased with MPC concentration of >0.67 mol/L (Fig. 2). On the CLPE-*g*-MPC surface with MPC concentration of 1.00 mol/L, the untreated CLPE (unstained) surface was observed in the FM image (Fig. 6(b)). The present graft polymerization reacts with free radicals which is photo-induced by an ultraviolet-ray irradiation to benzophenone as radical initiator. On the other hands, some ultraviolet-ray irradiation energies directly make free radicals form methacryl acid group of MPC unit in monomer solution. When the MPC concentration in feed is high, In addition to graft polymerization between a radical on the surface of CLPE and the MPC monomer, a homo-polymerization is also caused simultaneously in the system. The free radicals not only facilitate direct grafting of MPC to CLPE, thereby forming C–C covalent bonding between the MPC polymer and CLPE substrate, but also make homo-polymerization of MPC as free polymer in solution. And it was thought that the movement of a monomer was hardly in a high-concentration polymer solution, because a high-concentration polymer solution was high viscosity. When the monomer and the initiator attached surface were added all together with an ultraviolet-ray irradiation, radicals can be formed freely on the CLPE surface at the beginning of polymerization, but the surface radicals can not be reacted at a latter stage of polymerization because the growing polymer radicals and/or grafted polymer chains block the diffusion of radicals to the CLPE surface.[38] We therefore thought that the untreated CLPE surface appeared due to a decrease of MPC by a graft polymerization and a homo-polymerization.

In the case of a fixed irradiation time (polymerization time, 90 min in present study), a grafting efficiency (the content of nitrogen and phosphorous) in the CLPE-*g*-MPC surface increased with an increase to 0.50 mol/L MPC concentration, and then decreased with over 0.67 mol/L MPC concentration. It was assumed that in case of low monomer concentration in feed (0 to 0.50 mol/L), a rate of MPC homo-polymerization was higher than a rate of MPC graft-polymerization, and in contrast, in case of high monomer concentration in feed (>0.67 mol/L), a rate of MPC graft-polymerization was higher than a rate of MPC homo-polymerization, as trade-off. Moreover, although the rate of MPC graft-polymerization increased with an increase MPC concentration, the whole polymerization system began gel formation with MPC concentration of >0.67 mol/L and the grafting efficiency became low. In Fig. 1, when the irradiation time was greater than 45 min, the phosphorous concentration of the CLPE-*g*-MPC with various MPC concentrations became constant at

the high values. In order to obtain an poly(MPC) layer with high density, the irradiation time must be controlled in the previous study[12] The density of the poly(MPC) chains on the surface of the CLPE gradually increased with an increase of irradiation time and the entire surface of the CLPE was grafted using polymerization times longer than 45 min (approximately 90 min in the present study). It therefore became clear from the above result that it was necessary to perform a long irradiation time (polymerization time) to the polymerization system which contained a high-concentration monomer before its gelation, to obtain a CLPE-*g*-MPC with highly grafting efficiency.

In our previous studies, the mechanism of wear reducing was reported.[10-13] Since MPC is a highly hydrophilic compound, poly(MPC) is water-soluble. The water-wettability of the CLPE-*g*-MPC surface was considerable greater than that of an untreated CLPE surface. Therefore, the artificial hip joint bearing with the grafted MPC polymer surface exhibited considerably higher lubricity than that without the MPC polymer. In Fig. 8, we found that the water-wettability (static water-contact angle) was corresponded to the coefficient of friction. The significant reduction in the coefficient of friction of the grafted MPC polymer resulted in a substantial improvement in wear resistance.[10, 13] We assumed that the bearing surface of the artificial hip joint combined with MPC polymer exhibited the fluid film lubrication (or mixed lubrication) of the intermediate hydrated layer; this suggests that this novel artificial hip joint mimics the natural joint cartilage. It was probably assumed that the fluid-film (water-film) formability of poly(MPC) layer 10 nm thick was as well as that of poly(MPC) layer 10 μm thick. It was confirmed from the hip joint simulator test that the wear rate was much lower in the CLPE-*g*-MPC cups than in the untreated CLPE cups (Fig. 9). Since MPC is a highly hydrophilic compound, the water-wettability of the CLPE-*g*-MPC surface was greater than that of the untreated CLPE surface because of the poly(MPC) nano-layer. The orthopaedic bearing with an CLPE-*g*-MPC surface by 0.25 mol/L MPC concentration had high lubricity due to support a thin film of water as long as it has a poly(MPC) layer 10 nm thick. It is assumed that the poly(MPC) layer 10 nm thick is responsible for the improved wear resistance, and the wear resistance does not depend on its thickness. When CLPE surface is modified by poly(MPC) grafting, MPC graft polymer leads to a significant reduction in sliding friction between the surfaces to which are grafted, because water thin films formed can act as extremely efficient lubricants. The nano-scale modifications of poly(MPC) might be possible to brings to ultra-longevity for orthopaedic bearings. Moreover, we especially assumed that the grafting of poly(MPC) with 0.50 mol/L MPC concentration was essential to maintain the wear-resistance of CLPE-g-MPC as an orthopedic bearing material over long periods of time.[11]

CONCLUSION

The present study investigated the properties of the poly(MPC) layer formed on the CLPE surface by photo-induced radical graft polymerization, and the wear resistant properties of the CLPE-*g*-MPC were discussed in terms of the characteristics of the poly(MPC) nano-scale layer. It was confirmed from the hip joint simulator test that the wear rate was much lower in the CLPE-*g*-MPC cups than in the untreated CLPE cups. Since MPC is a highly hydrophilic compound, the water-wettability of the CLPE-*g*-MPC surface was greater than that of the untreated CLPE surface because of the poly(MPC) nano-scale layer. The orthopaedic bearing with an CLPE-*g*-MPC surface had high lubricity as long as it has a poly(MPC) layer 10 nm thick. Such poly(MPC) layer 10 nm thick is assumed to be responsible for the improved wear resistance. By changing the MPC concentration in feed, the thickness of poly(MPC) layer could be controlled. We concluded that the nano-scale modification of poly(MPC) could bring to ultra-longevity for orthopaedic bearings. And, it was necessary to perform a long irradiation time to the polymerization system which contained a high-concentration monomer before its gelation, to obtain this ultimate nano-scale modification of poly(MPC).

Acknowledgements

This work was supported by a Grant-in-Aid for Scientific Research (#15390449) from the Japanese Ministry of Education, Culture, Sports, Science and Technology and a Health and Welfare Research Grant for Traslational Research from the Japanese Ministry of Health, Labour and Welfare. The authors further express special thanks to Dr. Masaru Ueno, Mr. Yoshiki Ando, Mr. Noboru Yamawaki, Mr. Makoto Kondo and Mr. Takatoshi Miyashita (Japan Medical Materials Corp., Osaka, Japan) for their excellent technical assistance.

References

1. Iwasaki Y, Ishihara K. Phosphorylcholine-containing polymers for biomedical applications. Anal Bioanal Chem 2005;381(3):534–46.
2. Binyamin G, Shafi BM, Mery CM. Biomaterials: a primer for surgeons. Semin Pediatr Surg. 2006;15(4):276–83.
3. Kurtz S, Mowat F, Ong K, Chan N, Lau E, Halpern M. Prevalence of primary and revision total hip and knee arthroplasty in the United States from 1990 through 2002. J Bone Joint Surg Am 2005;87(7):1487–97.
4. Harris WH. The problem is osteolysis. Clin Orthop 1995;311:46–53.
5. Sochart DH. Relationship of acetabular wear to osteolysis and loosening in total hip arthroplasty. Clin Orthop 1999;363:135–50.
6. Oonishi H, Clarke IC, Good V, Amino H, Ueno M. Alumina hip joints characterized by run-in wear and steady-state wear to 14 million cycles in hip-simulator model. J Biomed Mater Res A. 2004;70(4):523–32.
7. McMinn DJ, Daniel J, Pynsent PB, Pradhan C. Mini-incision resurfacing arthroplasty of hip through the posterior approach. Clin Orthop Relat Res 2005;441:91–8.
8. Muratoglu OK, Bragdon CR, O'Connor DO, Jasty M, Harris WH. A novel method of crosslinking ultra-high-molecular-weight polyethylene to improve wear, reduce oxidation, and retain mechanical properties. Recipient of the 1999 HAP Paul Award. J Arthroplasty 2001;16(2):149–60.
9. Kyomoto M, Iwasaki Y, Moro T, Konno T, Miyaji F, Kawaguchi H, et al. High lubricious surface of cobalt-chromium-molybdenum alloy prepared by grafting poly(2-methacryloyloxyethyl phosphorylcholine). Biomaterials, in press.
10. Moro T, Takatori Y, Ishihara K, Konno T, Takigawa Y, Matsushita T, Chung UI, Nakamura K, Kawaguchi H. Surface grafting of artificial joints with a biocompatible polymer for preventing periprosthetic osteolysis. Nature Mater 2004;3:829–37.
11. Moro T, Takatori Y, Ishihara K, Nakamura K, Kawaguchi H. Grafting of Biocompatible Polymer for Longevity of Artificial Hip Joints. Clin Orthop Relat Res 2006;453:58–63.
12. Kyomoto M, Moro T, Konno T, Takadama H, Yamawaki N, Kawaguchi H, et al. Enhanced wear resistance of modified cross-linked polyethylene by grafting with poly(2-methacryloyloxyethyl phosphorylcholine). J Biomed Mater Res A, in press.
13. Kyomoto M, Moro T, Konno T, Takadama H, Kawaguchi H, Takatori Y, et al. Effects of photo-induced graft polymerization of 2-methacryloyloxyethyl phosphorylcholine on physical properties of cross-linked polyethylene in artificial hip joints. J Mater Sci Mater Med, in press.
14. Ishihara K, Ueda T, Nakabayashi N. Preparation of phospholipid polymers and their properties as polymer hydrogel membranes. Polym J 1990;22(5):355–60.

15. Ishihara K, Iwasaki Y, Ebihara S, Shindo Y, Nakabayashi N. Photoinduced graft polymerization of 2-methacryloyloxyethyl phosphorylcholine on polyethylene membrane surface for obtaining blood cell adhesion resistance. Colloids Surf B 2000;18:325–35.
16. Sibarani J, Takai M, Ishihara K. Surface modification on microfluidic devices with 2-methacryloyloxyethyl phosphorylcholine polymers for reducing unfavorable protein adsorption. Colloids Surf B Biointerfaces 2007;54(1):88–93.
17. Ueda H, Watanabe J, Konno T, Takai M, Saito A, Ishihara K. Asymmetrically functional surface properties on biocompatible phospholipid polymer membrane for bioartificial kidney. J Biomed Mater Res A. 2006;77(1):19–27.
18. Abraham S, Brahim S, Ishihara K, Guiseppi-Elie A. Molecularly engineered p(HEMA)-based hydrogels for implant biochip biocompatibility. Biomaterials 2005;26(23):4767–78.
19. Konno T, Hasuda H, Ishihara K, Ito Y. Photo-immobilization of a phospholipid polymer for surface modification. Biomaterials 2005;26(12):1381–8.
20. Palmer RR, Lewis AL, Kirkwood LC, Rose SF, Lloyd AW, Vick TA, Stratford PW. Biological evaluation and drug delivery application of cationically modified phospholipid polymers. Biomaterials 2004;25(19):4785–96.
21. Snyder TA, Tsukui H, Kihara S, Akimoto T, Litwak KN, Kameneva MV, Yamazaki K, Wagner WR. Preclinical biocompatibility assessment of the EVAHEART ventricular assist device: Coating comparison and platelet activation. J Biomed Mater Res A. 2007;81(1):85–92.
22. Kuiper KJ, Nordrehaug JE. Early mobilization after protamine reversal of heparin following implantation of phosphorylcholine-coated stents in totally occluded coronary arteries. Am J Cardiol 2000;85:698–702.
23. Ho SP, Nakabayashi N, Iwasaki Y, Boland T, LaBerge M. Frictional properties of poly(MPC-co-BMA) phospholipid polymer for catheter applications. Biomaterials 2003;24(28):5121–9.
24. Lewis AL, Hughes PD, Kirkwood LC, Leppard SW, Redman RP, Tolhurst LA, Stratford PW. Synthesis and characterisation of phosphorylcholine-based polymers useful for coating blood filtration devices. Biomaterials. 2000;21(18):1847–59.
25. Pavoor PV, Gearing BP, Muratoglu O, Cohen RE, Bellare A. Wear reduction of orthopaedic bearing surfaces using polyelectrolyte multilayer nanocoatings. Biomaterials 2006;27(8):1527-33.
26. Yamamoto M, Kato K, Ikada Y. Ultrastructure of the interface between cultured osteoblasts and surface-modified polymer substrates. J Biomed Mater Res 1997;37(1):29–36.
27. Wang P, Tan KL, Kang ET. Surface modification of poly(tetrafluoroethylene) films via grafting of poly(ethylene glycol) for reduction in protein adsorption. J Biomater Sci Polym Ed. 2000;11(2):169–86.
28. Iwata R, Suk-In P, Hoven VP, Takahara A, Akiyoshi K, Iwasaki Y. Control of nanobiointerfaces

generated from well-defined biomimetic polymer brushes for protein and cell manipulations. Macromolecules 2004;5(6):2308–14.

29. International Organization for Standardization 15989: Plastics - Film and sheeting - Measurement of water-contact angle of corona-treated films, 2004.
30. Wang JH, Bartlett JD, Dunn AC, Small S, Willis SL, Driver MJ, et al. The use of rhodamine 6G and fluorescence microscopy in the evaluation of phospholipid-based polymeric biomaterials. J Microsc. 2005;217(Pt 3):216–24.
31. ASTM F732-00: Standard test method for wear testing of polymeric materials used in total joint prostheses. In: Annual Book of ASTM Standards 13, 2004.
32. International Organization for Standardization 14242-1. Implants for surgery: Wear of total hip-joint prostheses Part 1: Loading and displacement parameters for wear-testing machines and corresponding environmental conditions for test, 2002.
33. International Organization for Standardization 14242-2. Implants for surgery: Wear of total hip-joint prostheses Part 2: Methods of measurement, 2000.
34. Matsuda T, Kaneko M, Ge S. Quasi-living surface graft polymerization with phosphorylcholine group(s) at the terminal end. Biomaterials 2003;24:4507–15.
35. Goda T, Konno T, Takai M, Moro T, Ishihara K. Biomimetic phosphorylcholine polymer grafting from polydimethylsiloxane surface using photo-induced polymerization. Biomaterials 2006;27(30):5151–60.
36. Braunecker WA, Matyjaszewski K. Controlled/living radical polymerization: Features, developments, and perspectives. Progress in Polymer Science, 2007;32(1):93–146.
37. Ma H, Davis RH, Bowman CN. A novel sequential photoinduced living graft polymerization. Macromolecules 2000;33(2):331–5.
38. Hegazy EA, Dessouki AM, El-Dessouky MM, El-Sawy NM, Crosslinked grafted PVC obtained by direct radiation grafting. Radiat Phys Chem 1985;26(2):143–9.

Figure captions

Figure 1. Phosphorus concentration as a function of irradiation time for CLPE-*g*-MPC.

Figure 2. Surface elemental concentration as a function of MPC concentration for CLPE-*g*-MPC.

Figure 3. Static water-contact angle as a function of MPC concentration for CLPE-*g*-MPC.

Figure 4. FT-IR/ATR spectra of CLPE-*g*-MPC with various MPC concentration.

Figure 5. Cross-section of TEM images of CLPE-*g*-MPC with various MPC concentration. Bar; 200 nm.

Figure 6. Fluorescence microscope images of CLPE-*g*-MPC with various MPC concentration. Bar; 20 μm.

Figure 7. Friction coefficients of CLPE-*g*-MPC surface as a function of MPC concentration.

Figure 8. Relationship between dynamic coefficient of friction and contact angle in CLPE-*g*-MPC surface. Bar; Standard deviations.

Figure 9. Weight change of CLPE-*g*-MPC cups polymerized with various MPC concentration in the hip joint simulation test. Bar; Standard deviations.

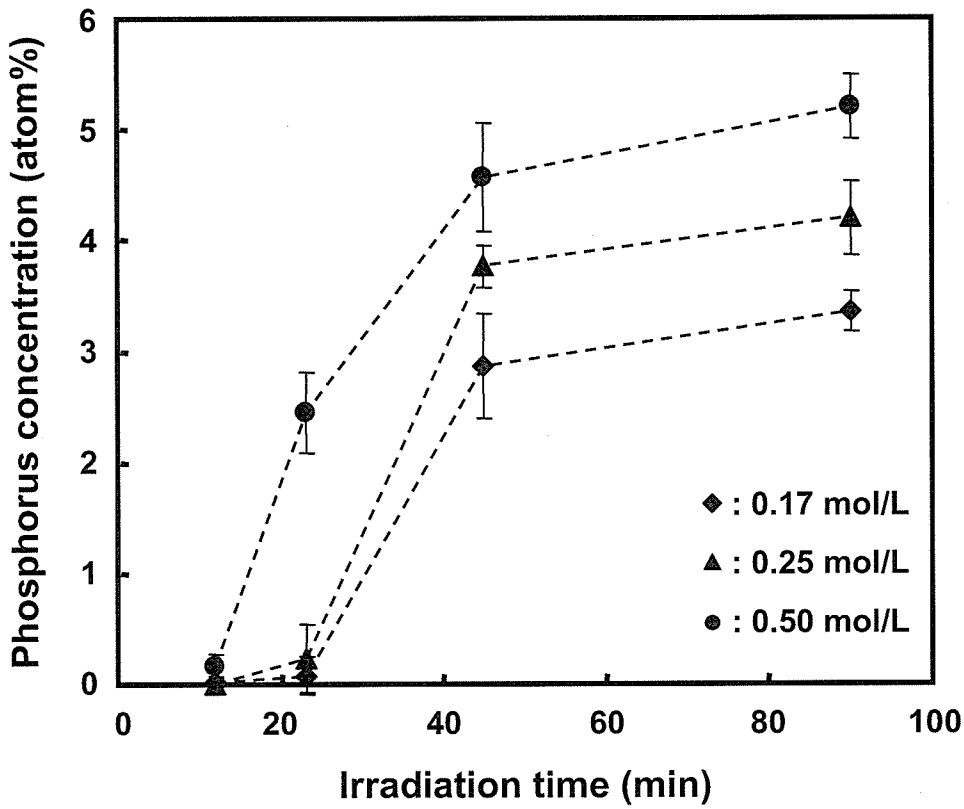

Fig. 1.
Phosphorus concentration as a function of irradiation time for CLPE-*g*-MPC.

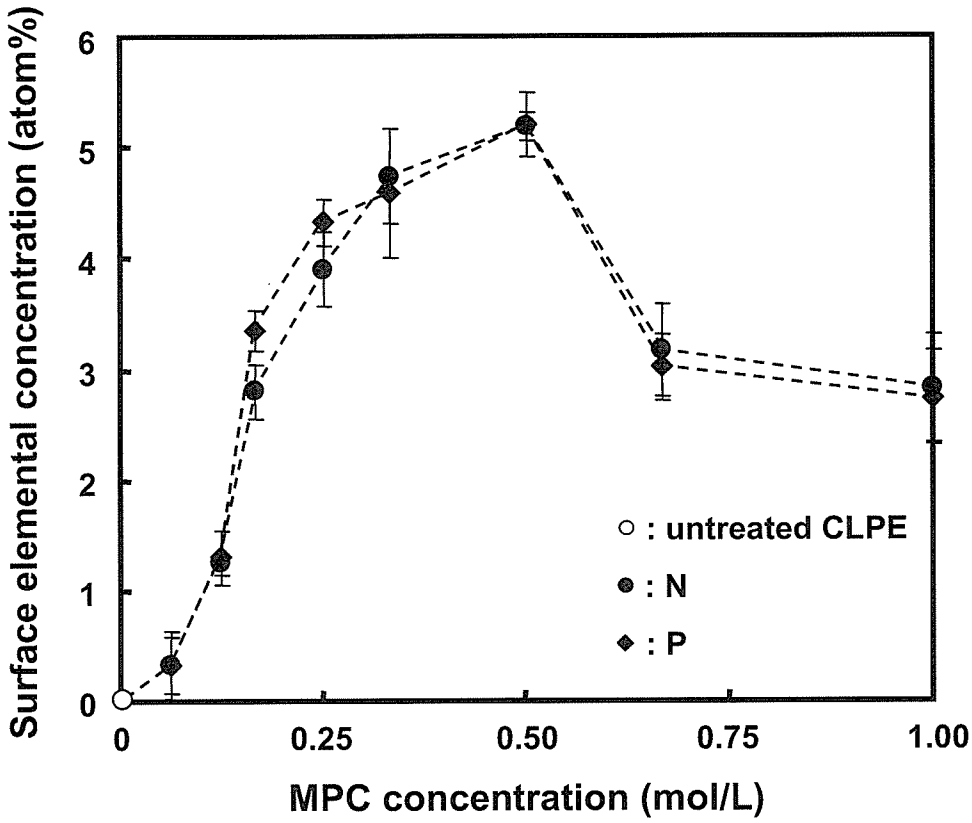

Fig. 2.
Surface elemental concentration as a function of MPC concentration for CLPE-*g*-MPC.

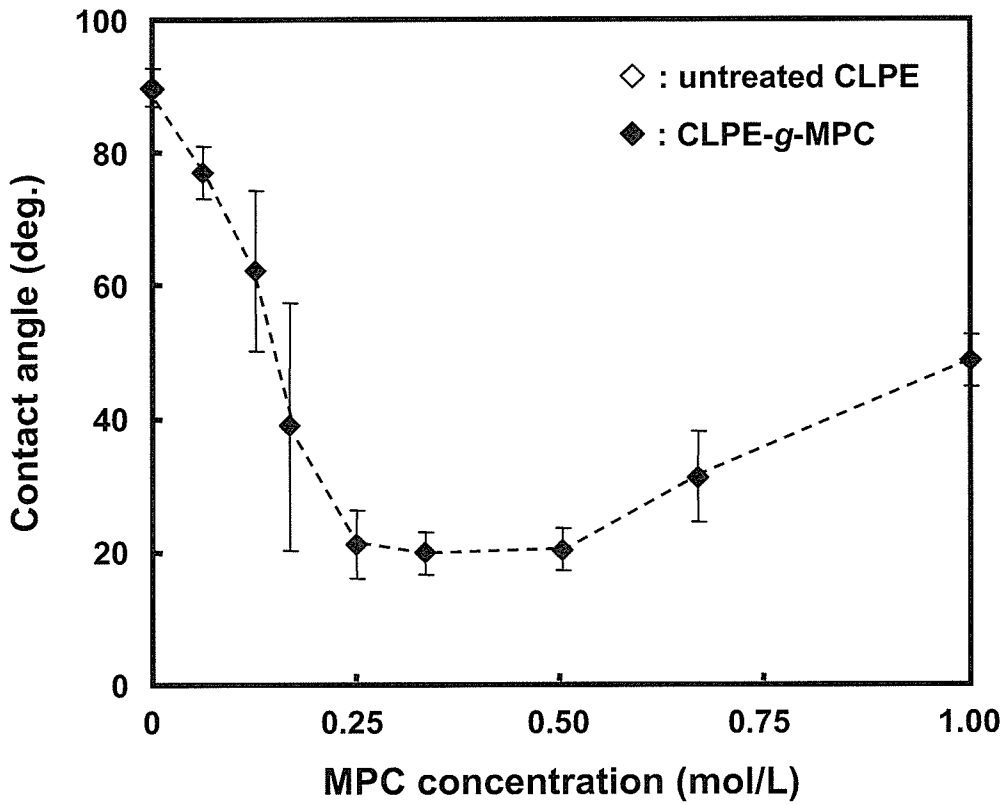

Fig. 3.
Static water-contact angle as a function of MPC concentration for CLPE-*g*-MPC.

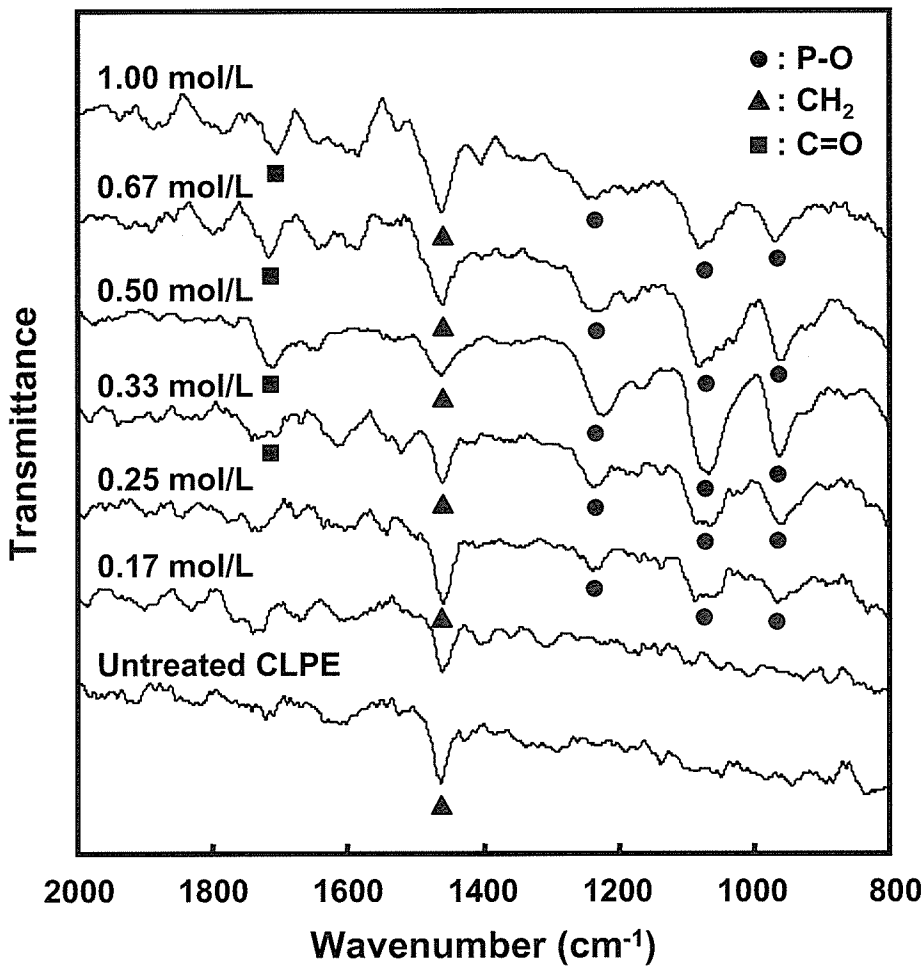

Fig. 4.
FT-IR/ATR spectra of CLPE-*g*-MPC with various MPC concentration.

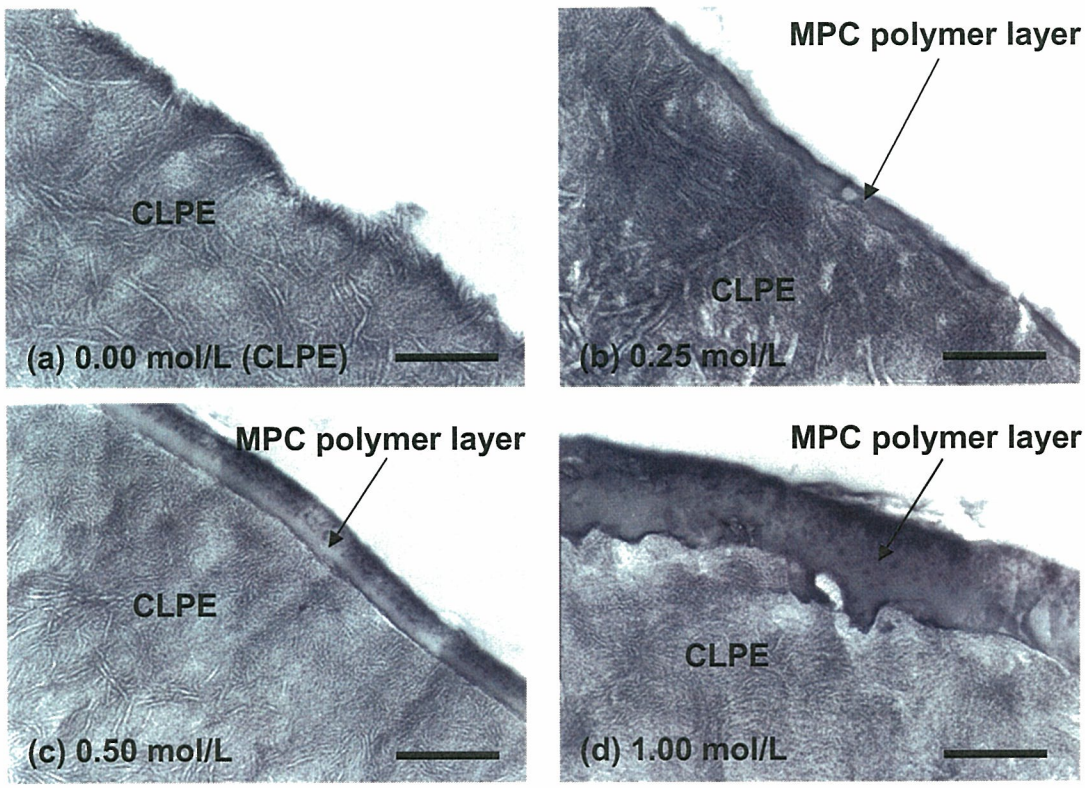

Fig. 5.
Cross-section of TEM images of CLPE-*g*-MPC with various MPC concentration. Bar; 200 nm.

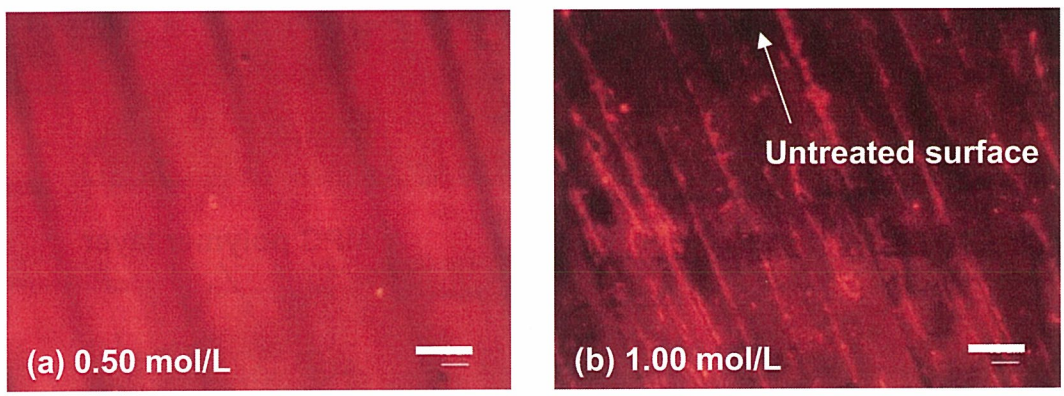

Fig. 6.
Fluorescence microscope images of CLPE-*g*-MPC with various MPC concentration. Bar; 20 μm.

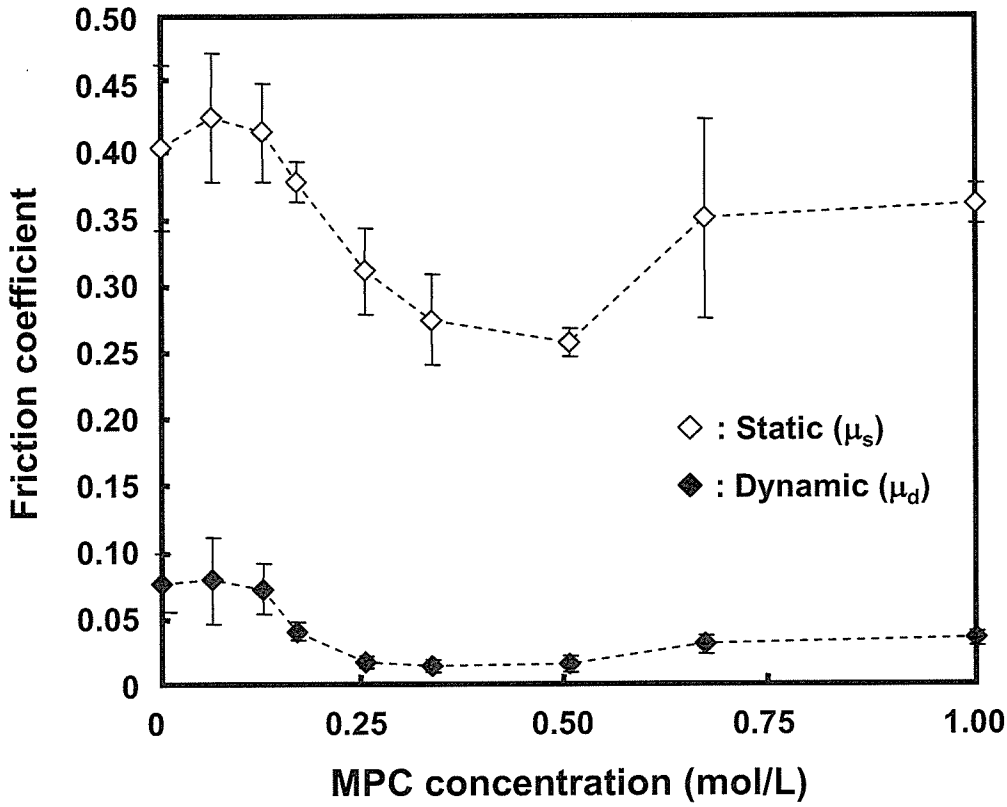

Fig. 7.
Friction coefficients of CLPE-*g*-MPC surface as a function of MPC concentration.

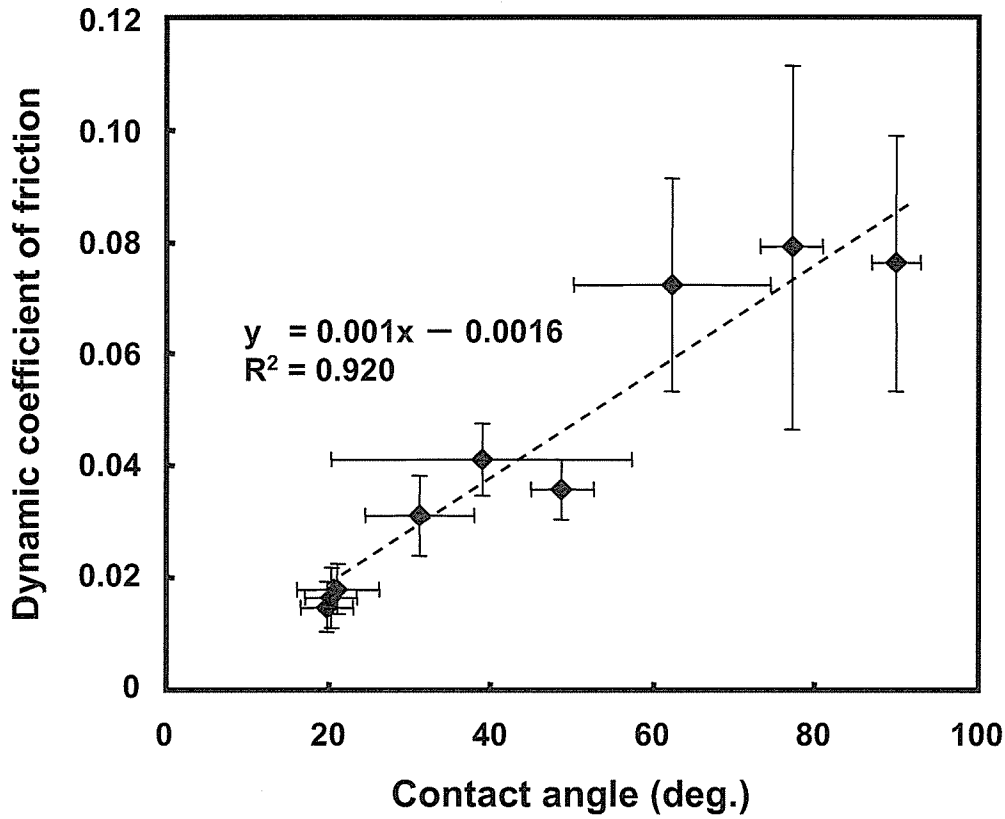

Fig. 8.
Relationship between dynamic coefficient of friction and contact angle in the CLPE-*g*-MPC surface.

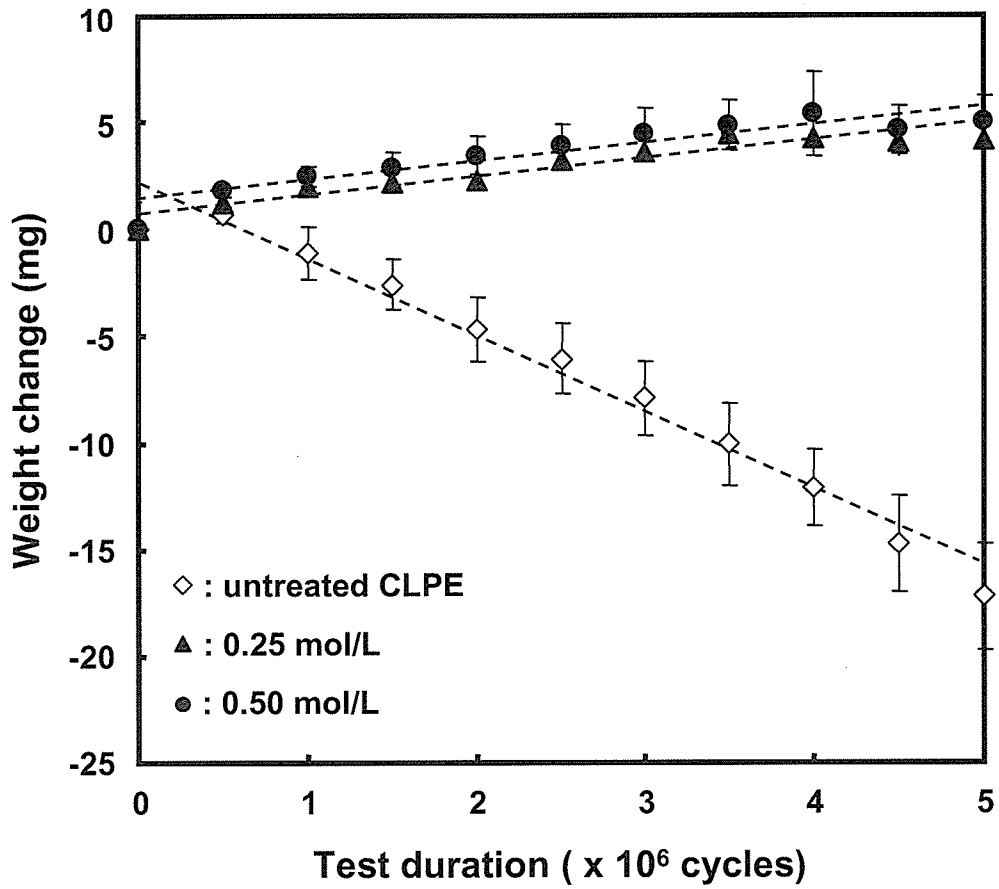

Fig. 9.
Weight change of CLPE-*g*-MPC cups polymerized with various MPC concentration in the hip joint simulation test. Bar; Standard deviations.